Variability in net ecosystem exchange from hourly to inter-annual time scales at adjacent pine and hardwood forests: a wavelet analysis

Authors: Paul C. Stoy, Gabriel G. Katul, Mario B. S. Siqueira, Jehn-Yih Juang, Heather R. McCarthy, Hyun-Seok Kim, A. Christopher Oishi, and Ram Oren

Stoy, Paul C., Gabriel G. Katul, Mario B. S. Siqueira, Jehn-Yih Juang, Heather R. McCarthy, Hyun-Seok Kim, A. Christopher Oishi, and Ram Oren (2005) Variability in net ecosystem exchange from hourly to inter-annual time scales at adjacent pine and hardwood forests: a wavelet analysis. Tree Physiology 25, no. 7: 887-902. DOI: 10.1093/treephys/25.7.887.

Variability in net ecosystem exchange from hourly to inter-annual time scales at adjacent pine and hardwood forests: a wavelet analysis

PAUL C. STOY,[1–3] GABRIEL G. KATUL,[1] MARIO B. S. SIQUEIRA,[1] JEHN-YIH JUANG,[1] HEATHER R. McCARTHY,[1] HYUN-SEOK KIM,[1] A. CHRISTOPHER OISHI[1,3] and RAM OREN[1]

[1] *Nicholas School of the Environment and Earth Sciences, Box 90328, Duke University, Durham, NC 27708-0328, USA*

[2] *Corresponding author (pcs3@duke.edu)*

[3] *University Program in Ecology, Duke University, Durham, NC, 27708, USA*

Summary Orthonormal wavelet transformation (OWT) is a computationally efficient technique for quantifying underlying frequencies in nonstationary and gap-infested time series, such as eddy-covariance-measured net ecosystem exchange of CO_2 (NEE). We employed OWT to analyze the frequency characteristics of synchronously measured and modeled NEE at adjacent pine (PP) and hardwood (HW) ecosystems. Wavelet cospectral analysis showed that NEE at PP was more correlated to light and vapor pressure deficit at the daily time scale, and NEE at HW was more correlated to leaf area index (LAI) and temperature, especially soil temperature, at seasonal time scales. Models were required to disentangle the impacts of environmental drivers on the components of NEE, ecosystem carbon assimilation (A_c) and ecosystem respiration (R_E). Sensitivity analyses revealed that using air temperature rather than soil temperature in R_E models improved the modeled wavelet spectral frequency response on time scales longer than 1 day at both ecosystems. Including LAI improved R_E model fit on seasonal time scales at HW, and incorporating parameter variability improved the R_E model response at annual time scales at both ecosystems. Resolving variability in canopy conductance, rather than leaf-internal CO_2, was more important for modeling A_c at both ecosystems. The PP ecosystem was more sensitive to hydrologic variables that regulate canopy conductance: vapor pressure deficit on weekly time scales and soil moisture on seasonal to interannual time scales. The HW ecosystem was sensitive to water limitation on weekly time scales. A combination of intrinsic drought sensitivity and non-conservative water use at PP was the basis for this response. At both ecosystems, incorporating variability in LAI was required for an accurate spectral representation of modeled NEE. However, nonlinearities imposed by canopy light attenuation were of little importance to spectral fit. The OWT revealed similarities and differences in the scale-wise control of NEE by vegetation with implications for model simplification and improvement.

Introduction

Net ecosystem exchange of CO_2 (NEE) is controlled by physical and biological processes that vary on multiple temporal scales (Olson et al. 1985, Berner and Lasaga 1989, Keeling et al. 1996, Baldocchi and Wilson 2001, Katul et al. 2001, Schimel et al. 2001, Gruber et al. 2002, Law et al. 2002). Thus, modeling NEE entails replicating measurements rich in spectral properties (e.g., Figure 1). Despite the complex controls on NEE and its components, ecosystem carbon assimilation (A_c) and ecosystem respiration (R_E), low-dimensional process-based models (i.e., models with few independent variables) remain desirable if prediction is accurately preserved. The challenge lies in creating models that are robust across the time scales of interest with simplifications that do not compromise the spectral characteristics of the model versus those of the measurements. Fourier and wavelet transformation are signal processing techniques used to quantify the spectral characteristics of data that vary across time or space, and are finding increasing application in the analysis and modeling of NEE time series (Baldocchi et al. 2001, Baldocchi and Wilson 2001, Katul et al. 2001, Katul and Siqueira 2002).

There are two primary complications to analyzing the spectral properties of eddy-covariance (EC)-measured NEE using standard Fourier transformation (FT). The first is that EC measurements are contaminated with missing data ("gaps") caused by rain events, calibration down-time and, often, the suppression of turbulent exchange at night (Falge et al. 2001). The second is that NEE time series are generally nonstationary (Scanlon and Albertson 2001), meaning that the statistical properties of NEE time series change over time (Hui et al. 2003). In contrast to FT, wavelet techniques can efficiently re-

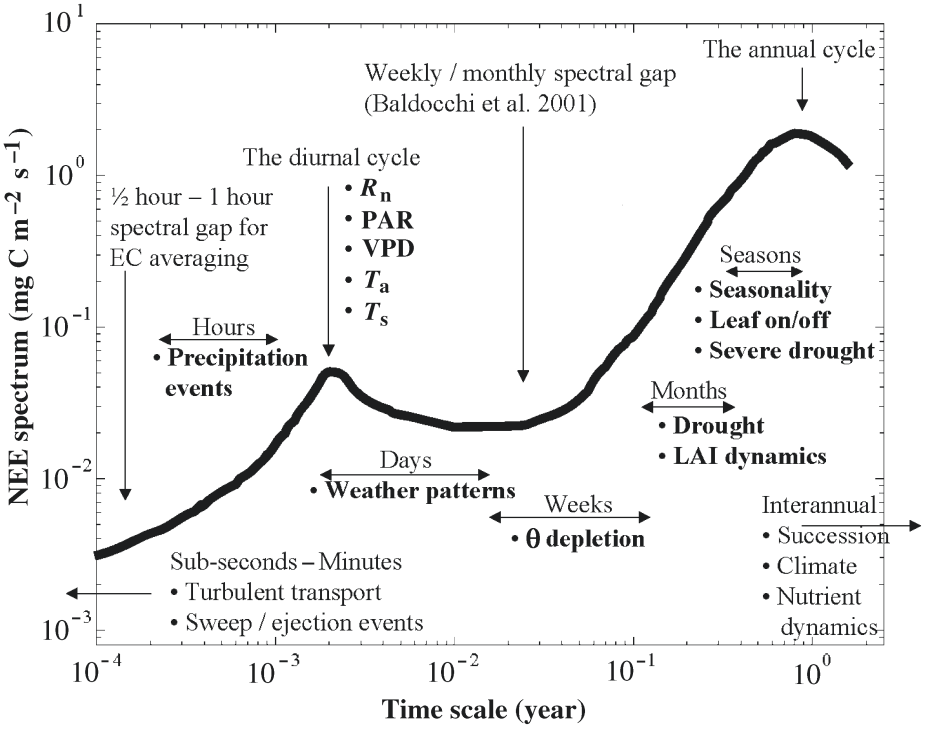

Figure 1. A conceptual description of the environmental drivers that impact net ecosystem exchange of CO_2 (NEE) at characteristic temporal scales. The abscissa is the time scale in units of years. Thus, 10^0 is 1 year, and the large signal in the NEE spectrum (the ordinate) represents variability from the annual cycle. Likewise, the peak at $10^{-2.56}$ years represents diurnal variability. The area under the curve is the variance of the NEE time series at each scale. Figures 4–9 have an identical abscissa and should be read in the same fashion as this figure. The factors in bold are considered in this analysis. Abbreviations: R_n = net radiation; PAR = photosynthetically active radiation; VPD = vapor pressure deficit; T_a = air temperature; T_s = soil temperature; and θ = volumetric soil moisture.

solve the contributions of processes that act on different frequencies in nonstationary and gap-infested EC-measured time series, and are thus a suitable tool for the interpretation and modeling of NEE (Katul et al. 2001). To date, wavelet analysis has not been used to compare the temporal responses of different ecosystems to common environmental drivers, or in conjunction with sensitivity analyses of process-based models.

Here, we employ orthonormal wavelet transformation (OWT) with the Haar basis function to analyze long-term (3.74 year) NEE measurements from a mid-rotation loblolly pine (*Pinus taeda* L.) plantation (hereafter PP) and a mature oak (*Quercus*)–hickory (*Carya*)-dominated hardwood forest (HW). These ecosystems are common on the landscape, serve as a model for succession in the southeastern US piedmont (Oosting 1942), lie adjacent to one another, and experience identical climatic and edaphic conditions. Thus, differential frequency responses to environmental drivers are due primarily to the effects of vegetation, and the motivation for this study was to understand temporal differences in the carbon dynamics of these typical southeastern U.S. ecosystems.

To illustrate, Figure 1 details key processes that are likely to affect a typical NEE spectrum on time scales from hours to years. Vegetation type is likely to alter the frequency distribution and the magnitude of the energetic modes at any given frequency. It is this response that should be captured by process-based models. Figure 2 describes the modeling approach taken here. Variability in environmental drivers, ecosystem characteristics and (potentially) model parameters are transferred by the model to modeled flux variability, which in turn is compared with the measured flux variability. The goal of this study was to find model transfer functions and parameterizations that capture this coupled physical/biological response on many time scales. Thus, our objective was to assess similarities and differences in how environmental and biological con-

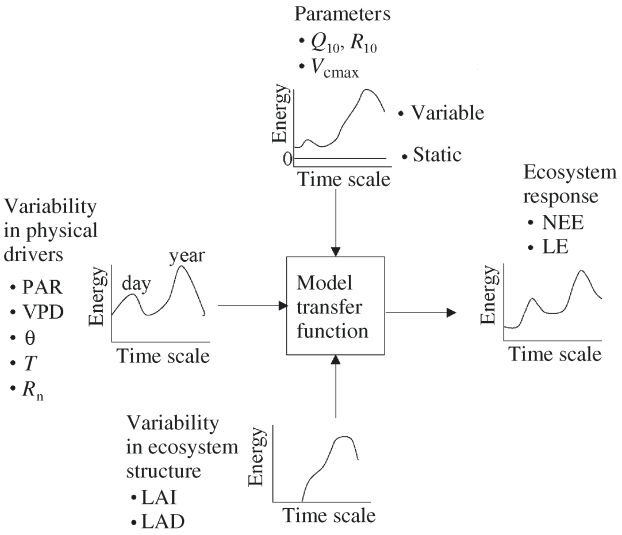

Figure 2. A schematic showing how models transfer variability across different time scales in physical drivers, ecosystem structure and model parameters to variability in fluxes. Here, variability is represented by the energy spectrum as a function of time scale as in Figure 1. Abbreviations: Q_{10} = ecosystem respiration sensitivity to temperature; R_{10} = reference respiration at 10 °C; V_{cmax} = maximum carboxylation efficiency; NEE = net ecosystem exchange of CO_2; LE = latent heat exchange; PAR = photosynthetically active radiation; VPD = vapor pressure deficit; θ = volumetric soil moisture; T = temperature; R_n = net radiation; LAI = leaf area index; and LAD = leaf area density.

trols modulate the NEE spectra of PP and HW by using a combination of data analysis, simplified models and sensitivity analysis.

We briefly contrast the principal strategies for spectral analysis, FT and wavelet transformation, with an example involving synthetic NEE time series. We then show that wavelet spectral and cospectral analysis of environmental and flux data alone is insufficient to isolate the mechanisms that control NEE at all time scales, but does uncover interesting correlations between NEE and environmental drivers at daily and seasonal time scales. The data analysis thus motivated a modeling study to isolate the role of intrinsic variability in physiological attributes (e.g., maximum carboxylation capacity (V_{cmax})) and canopy attributes (e.g., leaf area) from variability in environmental drivers on measured fluxes (see Figure 2). We used OWT to test if R_E, A_c and canopy stratification models of varying complexity replicate the variance of the measured flux signal at time scales from hours to years. After choosing the most robust R_E model structure, we added complexity to account for processes that act on seasonal to inter-annual time scales, such as the onset of drought and canopy leaf area. Conversely, we employed a sensitivity analysis to determine which environmental drivers most control the A_c component of NEE on time scales from hours to years. We note that a global analysis on such controls has already been conducted for various biomes (Law et al. 2002); however, an analogous scale-wise or spectral analysis has not been undertaken to date. The goal of the modeling approach was not to find models that replicate every half-hour flux measurement (in this case 65,536 or 2^{16} potential measurements); rather, it was to find simple models that capture the essential modes of NEE variability to deconvolve the important temporal differences in the carbon cycling function of the two ecosystems.

Materials and methods

Spectral analysis

A detailed description of OWT for flux applications is found in Katul and Parlange (1995). However, for completeness, we review the basic principles with hypothetical examples illustrating the effect of data gaps and time-frequency shifts (i.e., non-stationarity) to demonstrate the advantages of OWT over FT in the analysis of EC time series.

The purpose of spectral analysis is to quantify the underlying energetic (or active) frequencies in a signal that varies in time or space, or both. Fourier transformation, which remains the most popular tool for spectral analysis, separates or "decomposes" a signal into a series of sinusoidal functions of different frequencies such that when all squared amplitudes are summed, the original signal variance is recovered (Parseval's Identity).

Because the FT basis function is sinusoidal, rapid pulses and transients in the time series, e.g., the introduction of a gap or quick pulses caused by precipitation (Lee et al. 2004), affect all frequencies in the FT even though gaps and wetting events are localized and have clear physical time scales. Another difficulty with the sinusoidal basis function is a trend, linear or otherwise, which also affects all frequencies in the FT, a phenomenon known as red noise. Given that NEE time series are nonstationary (Scanlon and Albertson 2001), sinusoidal basis functions are not the optimum choice.

Wavelet transformation offers a reasonable solution to the aforementioned problems of discontinuity and nonstationarity by employing a finite basis function, called a mother wavelet, in the transformation. The mother wavelet is dilated (expanded and contracted) and translated across the signal and thus quantifies frequency as a function of time and scale. An infinite number of wavelet basis functions exist. The square-shaped Haar wavelet is ideal for analyzing spectral properties of NEE measurements because of its strong locality in the temporal domain (Katul and Parlange 1995, Katul et al. 2001, Scanlon and Albertson 2001) and for the accurate transformation of nonstationary and discontinuous data. An additional advantage of using wavelets for EC time series is that any time-independent bias in the EC measurements will not impact the spectral calculations because of the differencing properties of the wavelets.

In the graphical example in Figure 3, we introduce synthetic time series with "gaps" (Figure 3A) and non-stationarity (Figure 3B). The FT spectra of these signals are shown in Figures 3C and 3D, respectively. There are two distinct peaks in the FT spectra that correspond to the two dominant frequencies in the synthetic signal. Graphically, the sharp discontinuities in the time series (Figure 3A) add energy to the Fourier decomposition at multiple frequencies (Figure 3C). In contrast, the wavelet decomposition returns no measured variance when gaps in the synthetic signal occur (Figure 3E). Figure 3E is the wavelet "half-plane" that represents the frequency–time decomposition of the time series in Figure 3A using the Haar wavelet basis function. The OWT output in subsequent figures represents the mean of the wavelet coefficients at each power of two (excluding zero values generated by gaps) on the scale index (ordinate) of the wavelet half-plane.

For the nonstationary case, the FT in Figure 3D cannot readily determine where a shift in variance in the synthetic signal in Figure 3B occurs, which may be important to understanding ecosystem response to physical or biological drivers such as drought, or leaf-out at HW. The increasing variance of the nonstationary synthetic signal in (Figure 3B) is evident at the same times by a "whitening" of the wavelet half-plane (Figure 3F).

Practices designed to minimize the effects of non-stationarity on computing Fourier coefficients do so at the expense of accuracy. For example, employing short time FT to decompose nonstationary signals introduces errors near the edges of the moving windows that contain the sinusoidal basis function. Also, the size of the window remains arbitrary. Gap-filling techniques to obtain a continuous NEE data series (Falge et al. 2001) bias the spectral properties of NEE by the transfer function of the regression model or by constant values obtained from "look-up" tables.

The wavelet transform is continuous and the translation and dilation of the mother wavelet can occur at all points in the

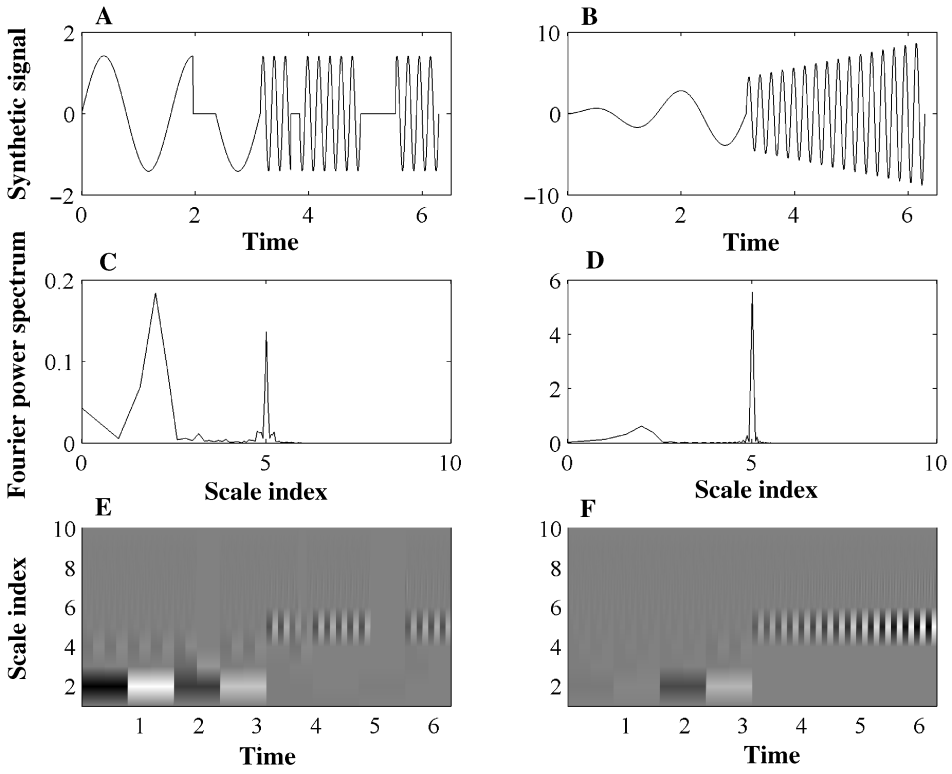

Figure 3. A synthetic time series with simulated gaps (A) and nonstationarity (B) with corresponding Fourier transformations (C, D) and discrete wavelet transformations with the Haar basis function, shown as the wavelet "half-plane" (E, F). The grayscale indicates the magnitude of the wavelet coefficients. The orthonormal wavelet transformation (OWT) output (Figures 4–9) represents the mean of the squared wavelet coefficients at each power of two (excluding zero values generated by gaps) on the "scale index" (ordinate) of the wavelet half-plane.

time series. However, discrete sampling is usually desirable to retrieve a tractable number of wavelet coefficients and to avoid redundant information. The OWT uses a log-spaced discretization while fully preserving measured variance in the flux signal. The OWT allocates most of the coefficients to the rapidly varying (high frequency) scales and less to slowly varying (low frequency) scales. Graphically, in Figures 3E and 3F, OWT coefficients represent the mean of the squared wavelet coefficients at each power of two. For a data series of length 2^N, OWT returns 2^N coefficients distributed across $N - 1$ time scales. Thus, the 3.74-year EC data records with 2^{16} measurements analyzed here result in 15 discrete orthonormal wavelet coefficients representing time scales from 30 min to 1.875 years.

Study sites

The PP and HW EC towers lie 750 m apart in the Blackwood Division of the Duke Forest near Durham, North Carolina (35°58′41.430" N, 79°05′39.087" W, 163 m a.s.l.). The experimental site also includes EC measurements at a grass-covered forest clearing, not considered here, and the three ecosystems serve as a model of post-agricultural ecosystem succession in the SE US Piedmont (Oosting 1942). The soils are Enon silt loam and Iredell gravelly loam, low-to-moderate fertility Hapludalfs found throughout the region. An impervious clay pan underlies the research sites at about 30 cm belowground (Oren et al. 1998). Mean growing season precipitation is 632 ± 130 mm and mean annual precipitation is 1145 ± 180 mm. The measurement period was characterized by an increasingly severe drought that extended from summer 2001 until October 2002. The April–September growing season precipitation was about 1 SD below average in 2001, about 2 SD below average in 2002, and about 1 SD above average in 2000 and 2003. Thus, the measurement period captures well the range of hydrologic conditions experienced by the ecosystems.

The PP was established in 1983 following a clear cut and burn and comprised primarily *P. taeda* with a minor component of *Liquidambar styraciflua* L. and a diverse understory. Ecosystem development has not been managed after planting. Mean canopy height increased from 16 to 18 m, and emergent treetops to 19 m, during the 3.74-year measurement period, another source of nonstationarity at PP. The HW is classified as an uneven-aged (80–100-year-old) oak–hickory forest with *L. styraciflua*, and *Liriodendron tulipifera* L. also contributing to the canopy and similar understory species as at PP. Mean canopy height at HW was 25 m with some emergent treetops reaching to 35 m. More detailed descriptions of PP and HW can be found elsewhere (Ellsworth 1999, Pataki and Oren 2003).

Eddy covariance measurements

Fluxes of CO_2 and H_2O were measured with EC systems comprising triaxial sonic anemometers (CSAT3, Campbell Scientific, Logan, UT) and open-path gas analyzers (LI-7500, Li-Cor, Lincoln, NE) positioned above the canopy at 20.2 m at PP and 39.8 m at HW. Covariances were computed for half-hourly periods, and spurious data were filtered as described by Katul et al. (1997). A closed path gas analyzer (LI-6262, Li-Cor) was employed at PP before May 1, 2001. The Webb-Pearman-Leuning (Webb et al. 1980) correction for

the effects of air density fluctuations on flux measurement was applied to scalar fluxes measured with the open-path Li-Cor LI-7500. Nighttime data were filtered based on the atmospheric stability threshold (Novick et al. 2004), which filters nighttime data if atmospheric stability is not near-neutral and if the peak of the source-weight function of the flux footprint, calculated using the approximate analytical model of Hsieh et al. (2000), exceeds the ecosystem dimension. The analytical footprint model, and thus the atmospheric stability threshold, is sensitive to friction velocity, sensible heat and ecosystem dimension. The HW flux measurements became available in October 2000. The HW NEE data prior to October 2000 were padded with zeros until 2^{16} data points were obtained. For OWT analysis, it is common to pad time series with zeros until a power of two is reached for computational efficiency (Torrence and Compo 1998). These zero-padded coefficients can be identified and removed in the wavelet spectral and co-spectral analyses.

Micrometeorological measurements

Micrometeorological variables were sampled every second and averaged every half hour at both ecosystems. Net radiation (R_n; W m^{-2}) and photosynthetically active radiation (PAR; μmol photons m^{-2} s^{-1}) were measured at 22 m at PP and 45 m at HW with Q7 Fritschen-type net radiometers (REBS, Seattle, WA) and Li-Cor LI-190SA quantum sensors, respectively. Air temperature (T_a) and relative humidity (RH) were measured at about two thirds canopy height with HMP35C temperature/RH probes (Campbell Scientific). Soil temperature (T_s) was measured at 10-cm depth at both ecosystems in at least four locations. At PP, volumetric soil moisture (θ; cm^3 cm^{-3}) was measured at four locations around the tower with CS615 soil moisture sensors (Campbell Scientific) that integrate from 0 to 30 cm belowground. At PP, θ was taken to be the mean of these values. At HW, θ was measured with ThetaProbe soil moisture sensors Type ML1 (Delta-T Devices, Cambridge, U.K.) positioned at 10- and 25-cm depths at 12 locations near the tower. To obtain a single value for θ that is comparable to PP, mean θ was computed for the 10- and 25-cm depths and these two values were further averaged to obtain site-wide θ.

Leaf area index measurements

At PP, the contribution to leaf area index (LAI; m^2 m^{-2}) from *P. taeda* and understory trees was calculated based on needle or leaf elongation and litterfall measurements (Oren and Pataki 2001). At HW, LAI was determined with a Li-Cor LAI-2000 plant-canopy analyzer together with litterfall measurements. Leaf area density (LAD) was measured about once a month at about 1-m height increments at PP and at about 2-m increments at HW with a Li-Cor LAI-2000. The full protocol for determining LAI and LAD at PP can be found elsewhere (Oren and Pataki 2001, Pataki and Oren 2003).

Models

Ecosystem respiration We estimated R_E from nighttime EC measurements (taken here to be periods where $R_n < 0$) in the absence of A_c. We tested simple temperature-based R_E models for their ability to match the frequency characteristics of the measured R_E, and then adjusted the R_E models to account for drivers that vary on time scales where the basic models fare poorly.

The popular Q_{10} respiration model, originally proposed by van't Hoff (1884), has found wide applicability in soil and ecosystem respiration research (Raich and Schlesinger 1992, Winkler et al. 1996). For the Q_{10} model:

$$R_{EQ10} = R_{10} Q_{10}^{(T-10)10} \quad (1)$$

where R_{10} is the reference respiration rate at 10 °C and Q_{10} is R_E sensitivity to temperature. We tested the frequency response of this model against R_E measurements with both T_a (abbreviated $R_{EQ10}a$) and T_s ($R_{EQ10}s$) as the independent variable. Slaytor (1906) first found temperature dependence in the Q_{10} parameter (Lloyd and Taylor 1994), and these observations have subsequently been confirmed for soil and ecosystem respiration (Lloyd and Taylor 1994, Kirschbaum 1995, 2000, Swanson and Flanagan 2001). However, soil respiration predictions based on temperature-insensitive parameters do not differ from those produced by temperature-dependent parameters at PP and HW (Palmroth et al. 2005); thus we employed the Q_{10} model for this analysis. We also tested improvements to R_{EQ10} by adding terms to account for θ, LAI, assimilated carbon and parameter variability (e.g., Janssens and Pilegaard 2003). These models are listed in Table 1 and described in Appendix A.

Canopy carbon assimilation We defined A_c as the difference between daytime measured NEE and modeled R_E. We considered both single layer ("big leaf") and multilayer canopy assimilation schemes. In both cases, to a first approximation, A_c can be described by a Fick's law analogy:

$$A_c = g_c C_a \left(\frac{C_i}{C_a} - 1 \right) \quad (2)$$

where g_c is canopy conductance to CO_2, C_a is atmospheric CO_2 concentration, and C_i is mesophyll CO_2 concentration for the canopy or vertically averaged canopy layer.

This equation has three unknowns. The C_i/C_a ratio can be solved by employing a "closure" model, which models C_i/C_a using empirical relationships between stomatal function and environmental conditions. Multiple closure formulations exist (Katul et al. 2000), and we chose three to represent a range of simplifications and biophysical reality.

The simplest model, referred to as the Norman (1982) closure model, assumes a fixed ratio between C_i and C_a for the entire canopy:

$$\frac{C_i}{C_a} = N_c \quad (3)$$

Table 1. Ecosystem respiration models. Abbreviations: R_{10} = reference respiration at 10 °C; Q_{10} = ecosystem respiration sensitivity to temperature; T_a = air temperature; T_s = soil temperature; h = canopy height; NEE_{cum} = cumulative sum of net ecosystem exchange; θ = volumetric soil moisture; a, b, c, d, h, j and m = fitted parameters.

Abbreviation	Model	Equation
R_{EQ10a}	$R_{10}Q_{10}^{(T_a-10)/10}$	1
R_{EQ10s}	$R_{10}Q_{10}^{(T_s-10)/10}$	1
$R_{E\theta}$	$R_{10}Q_{10}^{(T_a-10)/10}f(\theta);\ f(\theta)=-\frac{1}{e}+\frac{\exp\left(-\left\lvert\left(\frac{\theta-a}{b}\right)^m\right\rvert\right)}{1-\frac{1}{e}}$	1, A1
R_{ELAI}	$R_{10}Q_{10}^{(T_a-10)/10}+c\mathrm{LAI}+d$	A2
R_{EAc}	$R_{10}Q_{10}^{(T_a-10)/10}+h\mathrm{NEE}_{cum}+j$	A3
R_{EVP1}	Same as Equation 1, R_{10} and Q_{10} parameters fit to global summer and winter periods	
R_{EVP2}	Same as Equation 1, R_{10} and Q_{10} parameters fit to each summer and winter independently	

This simplification is surprisingly robust and has been upheld by both ecophysiological measurements (Ehleringer 1993, Ellsworth 1999) and models (Baldocchi 1994).

The Ball-Berry model is perhaps the most commonly used closure model (Ball et al. 1987, Collatz et al. 1991). After adjustment for use in Equation 2 (Katul et al. 2000), it takes the form:

$$\frac{C_i}{C_a}=1-\frac{1}{m_B\mathrm{RH}} \tag{4}$$

where m_B is a dimensionless parameter meant to approximate both physiological responses and aerodynamic resistance at the leaf surface.

Because RH is a poor driving mechanism for stomatal response and gas exchange (Aphalo and Jarvis 1991, Monteith 1995, Campbell and Norman 1998), Leuning (1995) modified the Ball-Berry model to account for a more appropriate driving variable, vapor pressure deficit (VPD):

$$\frac{C_i}{C_a}=1-\frac{1-\frac{\Gamma}{C_a}}{m_L}\left(1+\frac{\mathrm{VPD}}{D_o}\right) \tag{5}$$

Here, m_L is analogous to the Ball-Berry m_B, Γ is the leaf CO_2 compensation point, and D_o accounts for species-specific sensitivity to VPD.

The other unknown in Equation 2 is g_c. We modeled g_c using published relationships of stomatal sensitivity to PAR and VPD (Oren et al. 1999) that include data from PP and HW, with an adjustment for soil water limitations:

$$g_c=\frac{1}{1.6}(m_{PAR}\mathrm{PAR}+g_{PAR})(1-m\log\mathrm{VPD})g(\theta)\mathrm{LAI} \tag{6}$$

The first term converts stomatal conductance to H_2O to stomatal conductance to CO_2 by correcting for differences in molecular diffusivity, and m_{PAR} and g_{PAR} are fitted parameters. Multiplying by LAI converts stomatal conductance to g_c. Parameter m is about 0.6 for a wide range of temperate plant canopies including PP and HW (Oren et al. 1999), and $g(\theta)$ is a standard soil moisture reduction function:

$$g(\theta)=\begin{cases}1 & \frac{\theta}{\theta_R}>1\\ 1-\left(\frac{\theta_R-\theta}{\theta_R}\right)^v; & \frac{\theta}{\theta_R}\le 1\end{cases} \tag{7}$$

where θ_R is the value at which θ begins to limit g_c (Lai and Katul 2000, Novick et al. 2004) and v describes the curvature of the reduction function. For the single-layer canopy representation, A_c (Equation 2) can be solved for directly by combining Equation 6 with Equations 3, 4, or 5.

To simplify the sensitivity analysis, all parameters for the respiration, canopy conductance and single-layer A_c models were fit to the entire data sets by nonlinear optimization using the Gauss-Newton algorithm standard in MATLAB, unless otherwise stated. Initial parameter estimates were taken from literature sources where possible.

Sensitivity analysis

It is difficult to measure all biophysically important variables across time and space, and it is uncertain if the variability of all environmental drivers contributes to the observed flux variability (see Figure 2). To explore potential model and measurement simplifications, we performed a sensitivity analysis on single-layer A_c models by replacing measured variability with the global mean of PAR, VPD, θ and LAI (using maximum LAI for HW models).

In the context of the sensitivity analysis, simple multilayer canopy models, with varying simplifications to the LAD pro-

file, were examined to test if more detailed model transfer functions are necessary (Figure 2) and to investigate the importance of nonlinear responses of A_c to the light environment of the canopy in wavelet space. We also examined the importance of including temperature and time dependence of the parameters that describe the biochemistry of photosynthesis, namely V_{cmax}, as potential model simplifications (Campbell and Norman 1998, Ellsworth 2000, Wilson et al. 2001; see Appendix B). For multilayer canopy models, we introduced the Farquhar biochemical model for A_c as a function of C_i (Appendix B) and solved a system of three equations with three unknowns (A_c, g_c and C_i) at each canopy layer. We chose a layer height of 1 m for both ecosystems. Thus, the number of canopy layers increased from 15 to 19 at PP over the data record, and 38 canopy layers were used to describe HW. The canopy layering scheme included emergent trees. Spatial heterogeneity at HW was simplified by using mean LAI-2000 measurements from four directions at each canopy layer and only vertical LAD stratification was considered.

Although g_c places an important constraint on A_c (Schäfer et al. 2003), the system of equations in the multilayer model does not independently constrain A_c by g_c when g_c is low. Thus, after solving for multilayer A_c using Equations 2 and B1–B3, and the Leuning closure model (Equation 5), we adjusted multilayer modeled g_c with bulk canopy modeled g_c (Equation 6) and re-calculated A_c (Schäfer et al. 2003). Hence, the multilayer model only retains the nonlinearities of the leaf A_c with PAR relationship so that the vertically averaged C_i/C_a accounts for this nonlinearity. The photosynthetic parameters of the Farquhar model were taken from the literature, and thus may be seen as a "forward" model parameterization. Unlike the canopy conductance and single-layer models, the Farquhar parameters do not take the fitted parameter step described above.

Results

Data analysis

We normalized the flux and meteorological time series to have zero mean and unit variance for the purposes of the data analysis (Katul et. al 2001). We defined A_c as negative according to the micrometeorological convention, so negative wavelet cospectra correspond to either correlation with A_c or anti-correlation with R_E. In the context of Figure 2, this analysis is a direct comparison with the environmental and biological drivers at the left and bottom of the figure, respectively, with the flux response on the right side of the figure.

At the daily time scale, the wavelet cospectrum between T_s and NEE was more negatively correlated at HW than at PP, but the wavelet cospectra between T_a and NEE were correlated to a similar magnitude at both ecosystems (Figures 4A and 4B). Both PAR and R_n were correlated to NEE at short time scales at each ecosystem, but the correlation was stronger at PP than at HW at time scales from 6 hours to 2 days. At the seasonal time scale, LAI, g_c and VPD were more negatively correlated to NEE at HW (Figures 4C and 4D). At both ecosystems, θ was positively correlated to NEE at the seasonal time scale, particularly at HW. This corresponds to either correlation between θ and R_E or anti-correlation with A_c if θ is higher during

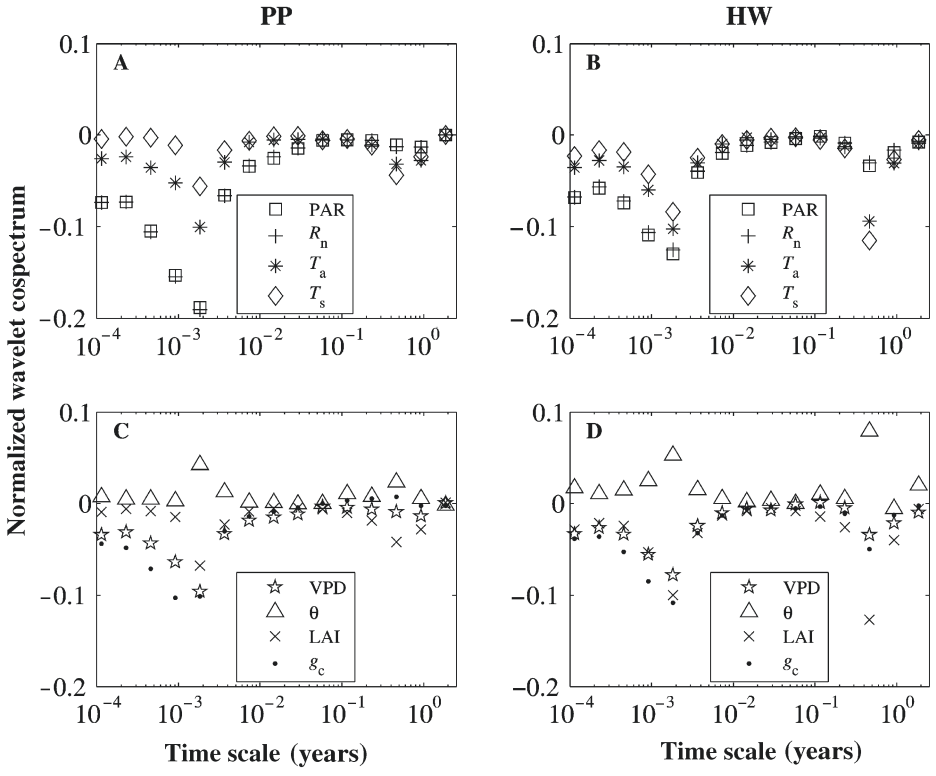

Figure 4. Normalized wavelet cospectra between net ecosystem exchange of CO_2 (NEE) and radiative environmental drivers at PP (A) and HW (B), and between NEE and hydrologic environmental drivers (C, D), noting that the two categories are not independent. The area under the normalized cospectrum represents the correlation coefficient between NEE and the signal analyzed. Abbreviations: PP = loblolly pine plantation; HW = mature oak–hickory dominated hardwood forest; R_n = net radiation; T_a = air temperature; T_s = soil temperature; PAR = photosynthetically active radiation; VPD = vapor pressure deficit; θ = volumetric soil moisture; LAI = leaf area index; and g_c = stomatal conductance.

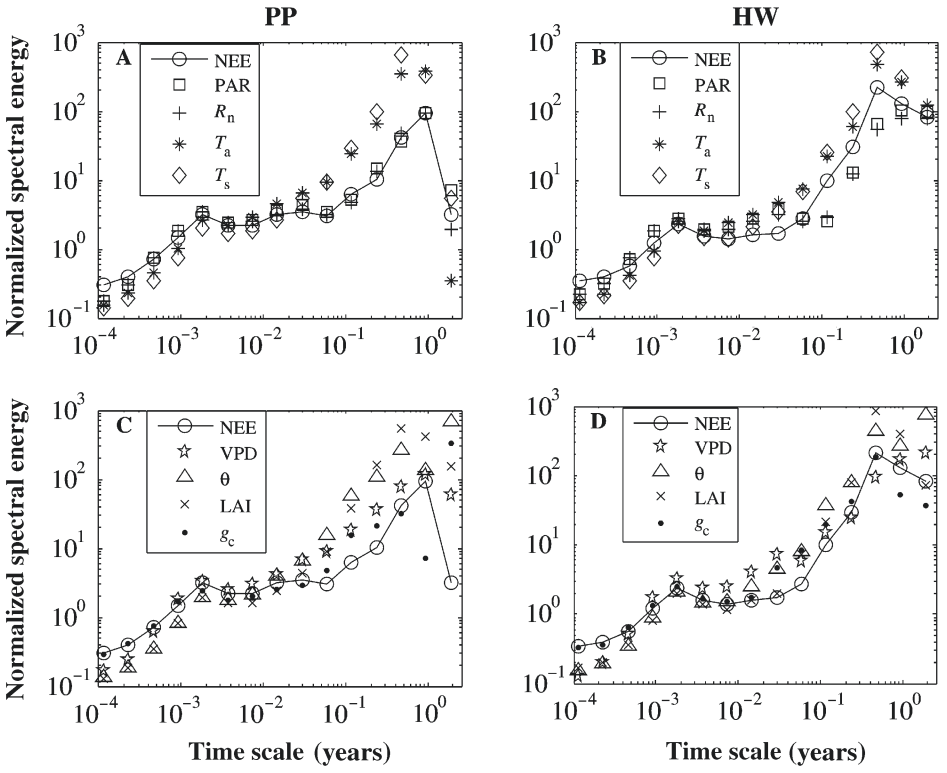

Figure 5. Normalized wavelet spectra of net ecosystem exchange of CO_2 (NEE) and radiative environmental drivers at PP (A) and HW (B), and between NEE and hydrologic environmental drivers (C, D), noting that the two categories are not independent. Abbreviations: PP = loblolly pine plantation; HW = mature oak–hickory dominated hardwood forest; PAR = photosynthetically active radiation; R_n = net radiation; T_a = air temperature; T_s = soil temperature; VPD = vapor pressure deficit; θ = volumetric soil moisture; LAI = leaf area index; and g_c = stomatal conductance.

winter periods with low assimilation, as was the case here.

Figure 5 shows that the seasonal variations in fluxes, environmental drivers and ecosystem characteristics dominated the overall variability of the time series. As expected, the wavelet-spectra of LAI showed more concentrated activity at the seasonal time scale at HW when compared with PP given the "square-wave" nature of the LAI dynamics at HW (versus sinusoidal at PP). Figure 5 also shows that hydrologic drivers including θ and VPD were more variable at PP than at HW at weekly to monthly time scales. If these drivers "resonate" with NEE at these scales, there may be differences in the hydrologic function of the two ecosystems.

Direct comparison of NEE spectra with those of environmental drivers (e.g., temperature) or intrinsic drivers (e.g., LAI) may be misleading, because it is unclear how driver variability "injects" variability in NEE through effects on A_c and R_E. For example, there was a strong seasonal spectral covariance between NEE and LAI (Figure 4), and the normalized wavelet spectra were similar at these time scales for both ecosystems (Figure 5). However, the cospectral and spectral relationship between NEE and LAI and NEE and temperature were similar (Figures 4 and 5). Clearly, variability in LAI and temperature impact NEE variability differently, but LAI and temperature are correlated. Models are necessary to deconvolve such impacts of environmental and intrinsic drivers on NEE and its components.

At PP, R_E exhibited no spectral gap on weekly to monthly time scales (Figures 6A and 6C) as observed with NEE measurements at this ecosystem (Figure 7) and in spectral analyses that employed the FT and flux gap filling (Baldocchi et al. 2001). Also, the spectral gap in NEE at weekly to monthly time scales was less pronounced at PP than at HW (Figure 7). This suggests that, at PP, R_E or A_c, or both, are sensitive to the drivers that act on these time scales, namely periodic θ depletion at the weekly time scale, or drought over monthly time scales (Figure 1). Again, models are necessary to examine the mechanistic bases for these responses. In the context of Figure 2, the following is an analysis of model transfer functions and their parameterizations.

Models

Ecosystem respiration Variability in R_E models did not match measured R_E variability on time scales shorter than about 1 month (i.e., 10^{-1} years, Figure 6). The R_{EQ10}a represented a minor improvement over R_{EQ10}s on most time scales except for sub-weekly time scales at HW (Figures 6A and 6B). Employing the suggested R_E model improvements (Table 1, Equations A1–A3) did not influence the model fit on hourly to monthly time scales at either ecosystem (Figures 6C and 6D). At PP, $R_{E\theta}$ (Table 1) improved interannual R_E model spectral response, and R_{EAc} (Table 1) improved both annual and interannual model spectral response. The R_{ELAI} (Table 1) gave better spectral fit on seasonal time scales at HW (Figures 6C and 6D). Parameterizing the Q_{10} model for each winter and summer season individually (i.e., R_{EVP2}) improved model fit on annual and interannual time scales at both ecosystems (Figures 6E and 6F). For simplicity, we retain R_{EQ10}a for NEE model analysis.

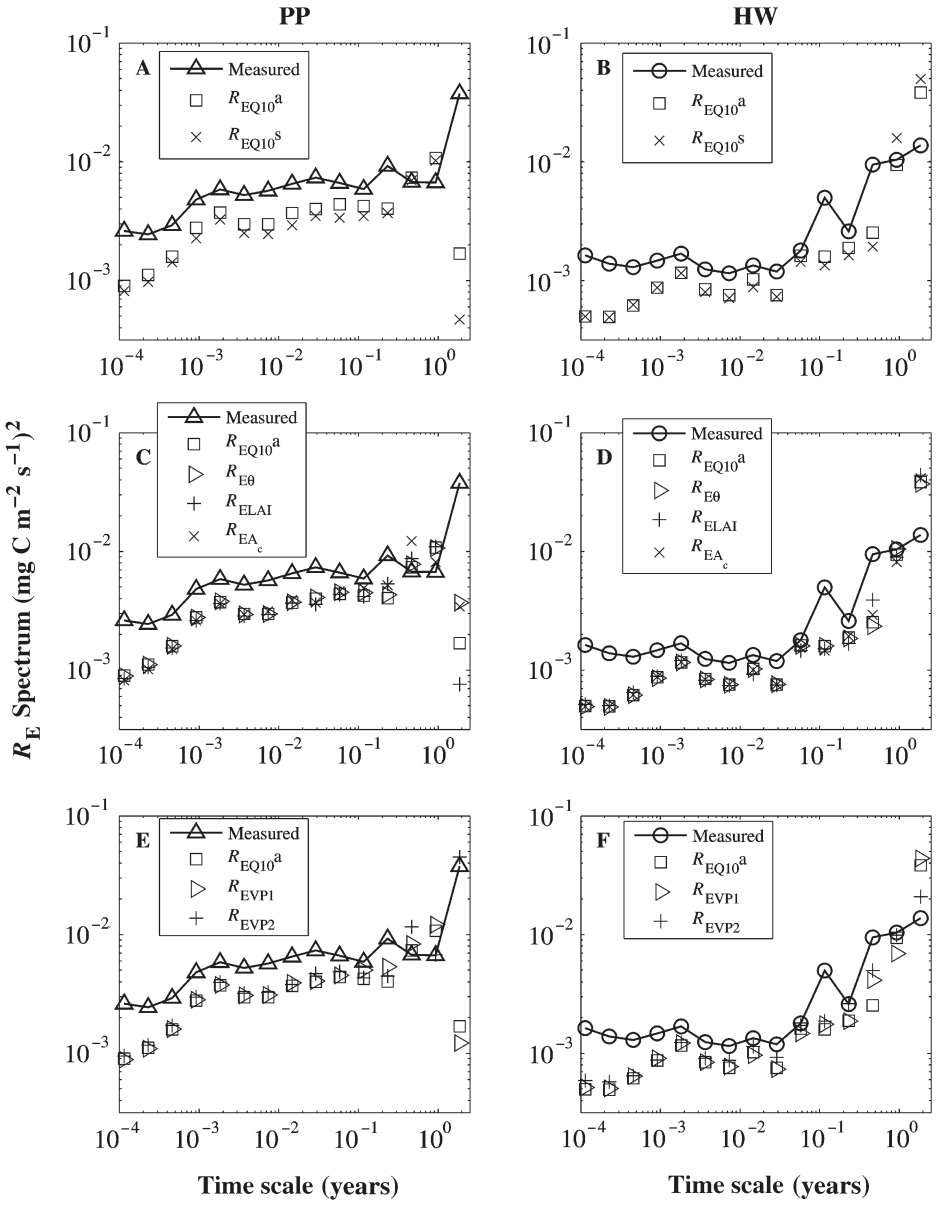

Figure 6. Wavelet spectral representation of measured and modeled R_E:Q_{10} models with air and soil temperature for PP (A) and HW (B). Wavelet spectral representation of ecosystem respiration (R_E) models with additional independent variables from Equations A1–A3 (C, D) and variable parameters (E, F) (see Table 1). Abbreviations: PP = loblolly pine plantation; HW = mature oak–hickory dominated hardwood forest; $R_{EQ10}a = Q_{10}$ model with air temperature; $R_{EQ10}s = Q_{10}$ model with soil temperature; $R_{E\theta} = Q_{10}$ model with soil moisture; $R_{ELAI} = Q_{10}$ model with leaf area; $R_{EA_c} = Q_{10}$ model with cumulative net ecosystem exchange for the prior 2-week period; $R_{EVP1} = Q_{10}$ model where the parameters are fit for combined summer and winter periods; and $R_{EVP2} = Q_{10}$ model where the parameters are fit for each summer and winter period separately. See Table 1 for model descriptions.

Canopy carbon assimilation Models generally matched measured NEE variability well, but the Ball-Berry closure model performed relatively poorly on time scales from 4 days to years at both ecosystems; the spectral energy of the Ball-Berry model did not match NEE measurements at these time scales (Figures 7A and 7B). Constant g_c resulted in poor model fit on almost all time scales at PP and on all sub-weekly time scales at HW (Figures 7A and 7B). At both PP and HW, there was little difference between the Norman and Leuning model spectra (Figures 7A and 7B), but the latter fit better on inter-annual time scales at PP. We retain the Leuning closure model for the sensitivity analysis, which is meant to quantify which environmental and biological drivers most impact observed NEE, as well as the complexity of transfer functions required to capture NEE measurement variability (Figure 2).

Sensitivity analysis

Photosynthetically active radiation was the most important input for NEE model fit on short (hourly to weekly) time scales at both ecosystems (Figures 7C and 7D); the wavelet coefficients in models without PAR variability did not match the peak node in measured NEE on the daily time scale. At PP, VPD was the most important model input on monthly to bimonthly time scales, θ on monthly time scales, and LAI on seasonal to interannual time scales. At HW, simplifying LAI by using its maximum value over-specified NEE model variability on multiple time scales (Figure 7D). The HW ecosystem was generally less sensitive to simplifications in VPD and θ than the PP ecosystem. However, NEE at HW was sensitive to θ on weekly time scales (Figure 7D), rather than on monthly time scales as at PP (Figure 7C).

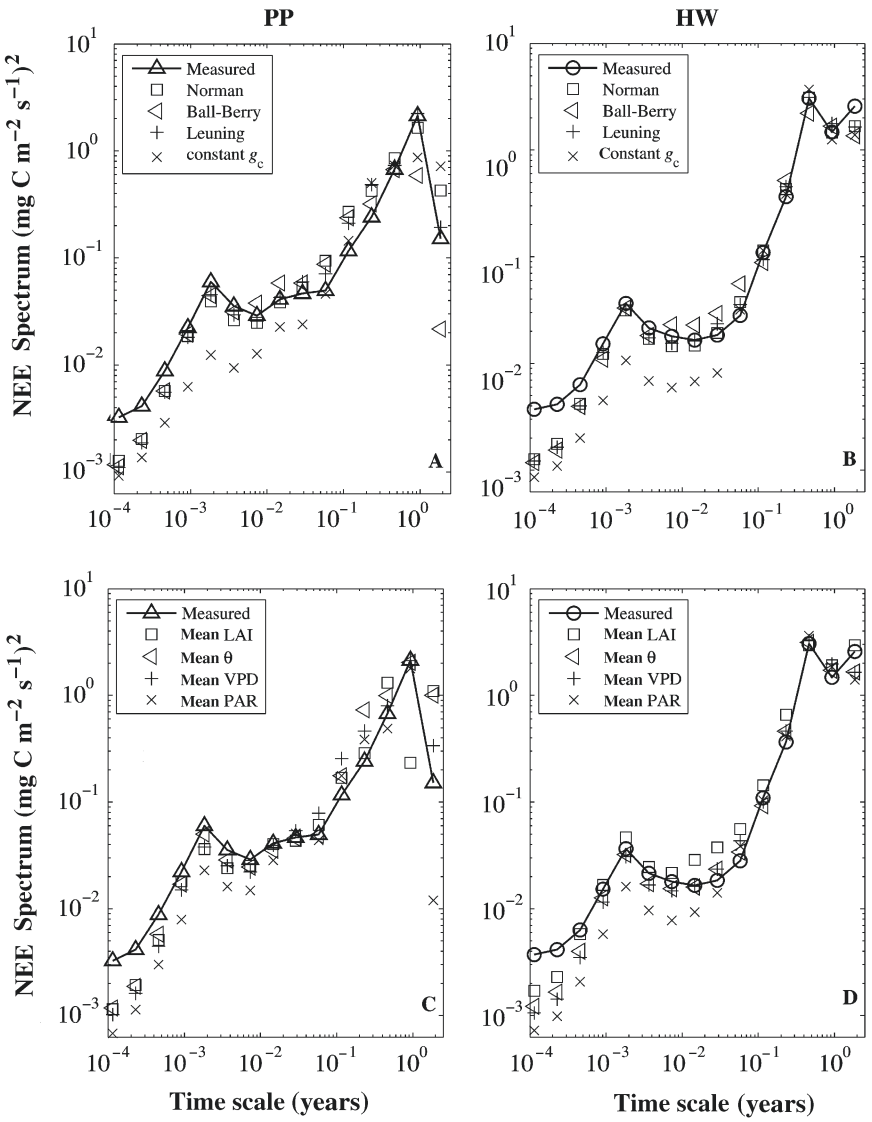

Figure 7. Wavelet spectral representation of single-layer ("big leaf") net ecosystem exchange (NEE) models with different closure schemes from Equations 3–5 (A, B) and simplifications to model input (C, D) (i.e., "mean VPD" means that mean vapor pressure deficit (VPD) is used and no measured VPD variability is input into the model. Abbreviations: PP = loblolly pine plantation; HW = mature oak–hickory dominated hardwood forest; g_c = canopy conductance to CO_2; LAI = leaf area index; θ = volumetric soil moisture; VPD = vapor pressure deficit; and PAR = photosynthetically active radiation.

Both ecosystems, particularly HW, were relatively insensitive to dramatic simplifications in LAD (Figures 8A and 8B) for modeling the C_i/C_a. Both PP and HW were sensitive to the assumption of temperature independence of the V_{cmax} parameter on all time scales longer than hours and days, respectively (Figures 8C and 8D). The HW ecosystem was more sensitive than the PP ecosystem to modeling the seasonal dynamics of V_{cmax} that result from leaf age (Ellsworth 2000, Wilson et al. 2001), particularly at weekly and monthly time scales.

Discussion

Data analysis

The peak in the wavelet cospectrum between PAR and NEE at the daily time scale at both ecosystems was an expected result of ecosystem light response. The stronger cospectral peak at the daily time scale at PP was due to the poor relationship between PAR and NEE during wintertime at HW; NEE at PP can still respond to PAR variability during the winter in the southeastern USA. The peaks in the cospectrum at the seasonal time scale between both NEE and LAI and NEE and g_c at HW were expected and correspond to the "on–off" LAI seasonality of the deciduous ecosystem. The stronger seasonal correlations between NEE and both T_a and T_s at HW than at PP were unexpected and the models will be used to investigate these responses.

Ecosystem respiration

At both ecosystems, the greater variability at half-hourly time scales than at hourly time scales reflects the intermittent nature of EC-measured R_E (Lee 1998), which may include storage and ejection of CO_2 from the canopy volume, the dynamic footprint that samples different vegetation patches depending on atmospheric conditions and wind direction, and measurement error in the EC systems (Goulden et al. 1996, Moncrieff et al. 1996). These are important sources of potential error

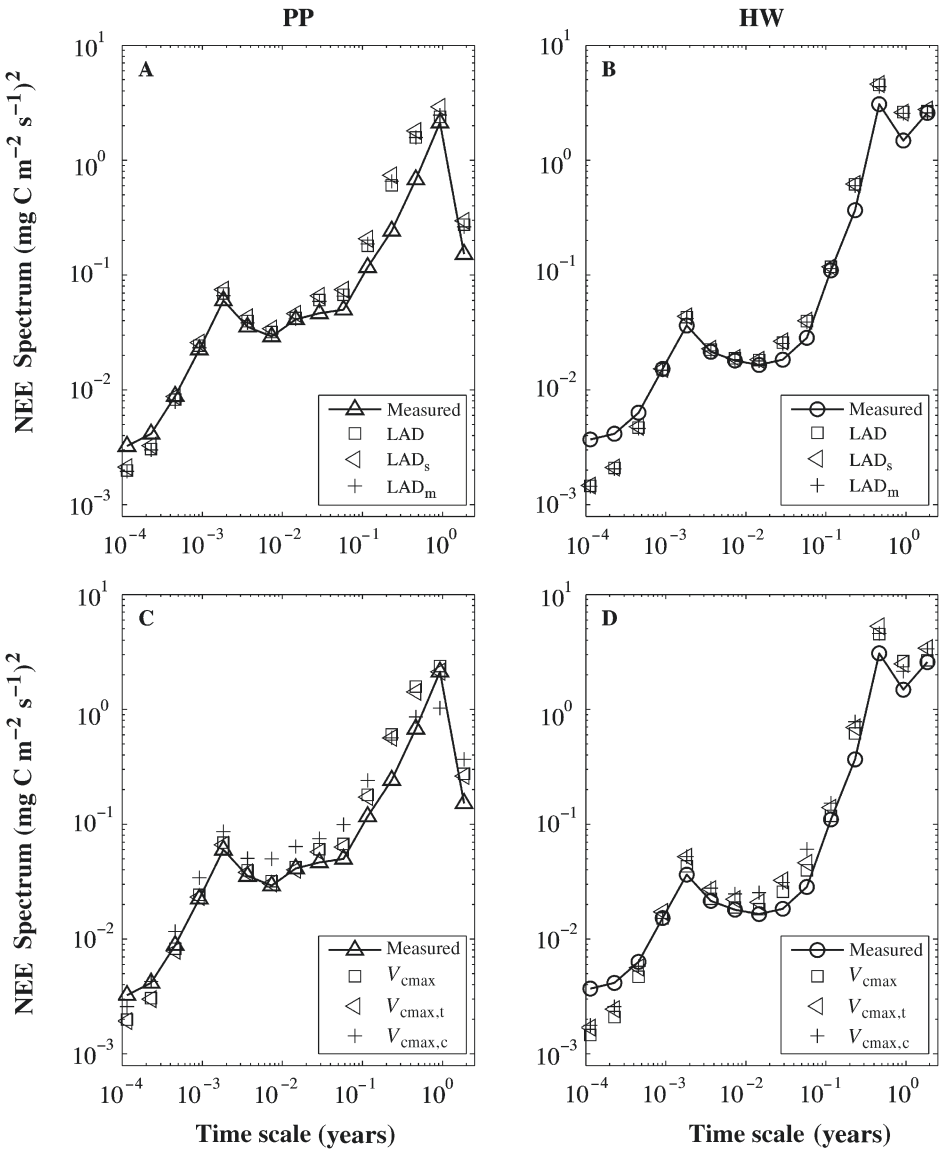

Figure 8. Wavelet spectral representation of multilayer net ecosystem exchange of CO_2 (NEE) models with simplifications in the vertical structure of the vegetation (A, B) and variability of the maximum carboxylation capacity (V_{cmax}) parameter (C, D). The abbreviation LAD refers to the model with measured leaf area density (LAD) that varies in time and space. Model LAD_s employs a simplified variation of LAD that varies in space but not with time. Model LAD_m is highly simplified and employs a constant LAD (= LAI/h, where h = canopy height) at each layer for all times. Model V_{cmax} employs a V_{cmax} parameter that varies seasonally and is sensitive to temperature. Model $V_{cmax,t}$ varies with temperature but not time, and model $V_{cmax,c}$ treats V_{cmax} as a constant. Abbreviations: PP = loblolly pine plantation; and HW = mature oak–hickory dominated hardwood forest.

(and perhaps bias) in interpreting the R_E component of EC-measured NEE at short time scales. The models did not include stochastic components to account for random measurement error and were not spatially explicit to consider effects of the variable footprint. If the patches of forest differ in either state variables (e.g., T_a, T_s, or θ) or sensitivity to the state variables (e.g., R_{10}, Q_{10}), then an ecological model with fixed parameters will always underestimate variability in measured R_E.

The PP ecosystem was sensitive to the drivers that act on weekly and monthly time scales as evidenced by the lack of spectral gap in measured R_E, but models did not capture variability at sub-monthly time scales at either PP or HW. Independent modeling studies (Schäfer et al. 2003) found that R_E at PP was sensitive to A_c, and $\delta^{13}C$ analysis (Andrews and Schlesinger 2001, Mortazavi et al. 2005) showed that this effect occurs on time scales of less than a week. However, adding A_c improved R_E model fit at PP only slightly on monthly, annual and interannual time scales. Thus, any potential coupling between A_c and R_E at sub-weekly time scales was overshadowed by other sources of variability in the EC measurements. However, variability in T_a better explained variability in R_E on short time scales, particularly at PP. These results further suggest that aboveground processes, including those that determine A_c, were important in controlling R_E at PP compared with HW. This analysis further supports the stable isotope analysis of Mortazavi et al. (2005), who showed that aboveground respiration contributes more to R_E at PP than at HW. For these ecosystems, sensitivity to T_s or T_a at short time scales can be a surrogate for determining how the aboveground fraction contributes to R_E.

In summary, models for EC-measured R_E can give the desired spectral response on time steps of months or longer if the proper driving mechanisms are included, but sub-monthly variation in R_E was not well captured in the widely used model formulations. We found that models with "improvements" (Equations A1–A3) often fared worse than simpler models, in-

dicating that adding model complexity does not necessarily improve model skill, at least in replicating the spectral response of EC-measured R_E. Simpler model transfer functions may improve spectral fit between models and measurements (see Figure 2). However, modeling parameter variability (e.g., R_{EVP2}) was an effective step in improving model fit to EC data on longer time scales. This suggests that simple hierarchical models with transient parameters, rather than complicated model transfer functions, may better describe R_E variability across time.

Canopy assimilation models

Models accurately replicated measured variability in NEE on daily to seasonal time scales despite the poor performance in replicating R_E. However, the Ball-Berry closure model generally gave a worse spectral fit than treating C_i/C_a as a constant (i.e., the Norman model) because of accumulated errors from employing a biophysically unrealistic descriptor of gas exchange, RH, in the model transfer function. This effect was particularly pronounced on longer time scales at PP, where vegetation is active during winter and VPD is lower regardless of RH because of low temperatures. Independent studies have shown the Ball-Berry model to be inadequate for modeling A_c at PP (Katul et al. 2000), and the results here extend this finding to longer temporal scales for two different ecosystems. Norman's assumption of a constant C_i/C_a was robust at most time scales in both ecosystems, and variability in g_c dominated variability in A_c. Thus, resolving variability in canopy conductance and not leaf biochemistry was the crucial step in accurately describing the spectral characteristics of NEE at PP and HW.

Sensitivity analysis

Our analysis suggests that resolving the temporal dynamics of all variable inputs at both ecosystems may be unnecessary to model the broad spectral response of NEE. For example, on time scales greater than four days, variability of NEE at PP can be explained by variability in VPD, θ and LAI alone, without variability in PAR (Figure 7C). Models of NEE at HW were generally amenable to simplifications in VPD, θ and PAR on time scales longer than weeks. The PP ecosystem was relatively more sensitive to hydrologic drivers (i.e., VPD and θ). Although HW and a similar forest were found to be relatively insensitive to hydrologic drivers, PP was found to be highly sensitive to these variables (Oren et al. 1998, Oren and Pataki 2001, Pataki and Oren 2003). This study additionally shows that NEE at PP is sensitive to θ at longer time scales than HW, and further analysis can clarify these responses.

Measured θ was never less than θ_R (Equation 7) during the wetter years (2000 and 2003) at either ecosystem. During periods with high PAR (> 1200 μmol m^{-2} s^{-1}) in the May–August peak growing season of the mild drought year (2001), θ_R was 0.17 m^3 m^{-3} at PP and 0.16 m^3 m^{-3} at HW (model parameters were otherwise fit to the entire data sets to simplify the sensitivity analysis). For the same periods in the severe drought year (2002), g_c at PP was slightly more sensitive to θ (θ_R = 0.19 m^3 m^{-3}), whereas θ_R at HW did not change. Parameter error is on the order of 0.005 m^3 m^{-3}. These parameter values are close to those calculated for a nearby grass clearing (θ_R = 0.19–0.20 $m^3 m^{-3}$) (Lai and Katul 2000, Novick et al. 2004), and alone suggest minor differences in the onset of drought sensitivity between the ecosystems. However, compared with HW, PP used water less conservatively and experienced longer periods for which $\theta < \theta_R$. This resulted in the observed sensitivity to θ on monthly and weekly time scales at PP and HW, respectively.

In 2001, θ was less than θ_R for 40% of the high PAR period (372 incidences/933 measurements) at PP, but only 10% of the time at HW (83/808). During the severe drought of 2002, θ was less than θ_R for nearly the entire peak growing season at PP (93%, 676/727), but less than half of the time at HW (46%, 444/968). Thus, variability in θ impacted HW for shorter periods during drought, and this response was elucidated by the model sensitivity analysis. Integrated over the course of a year, there were small differences in mean θ between PP and HW (Palmroth et al. 2005), but variability in θ has different temporal consequences for NEE in these ecosystems. Modeling efforts should reflect the central role of hydrologic variability on the variability of the terrestrial C cycle in temperate ecosystems (Ollinger et al. 1998, Schäfer et al. 2003), noting that adjacent, edaphically similar ecosystems may have different temporal responses to a common drought.

The PP ecosystem was sensitive to the constant V_{cmax} simplification at most time scales including annual and longer, reflecting the importance of capturing dynamic leaf responses to

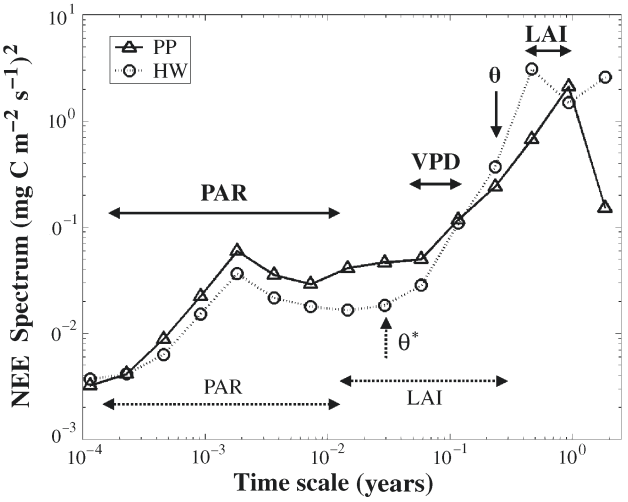

Figure 9. A graphical summary of the most important inputs for the net ecosystem exchange (NEE) models at PP (thick line) and HW (thin line) as determined by spectral sensitivity analysis. This figure is not meant to exclude the importance of drivers at certain time scales; for example, vapor pressure deficit (VPD) variability is an important input for NEE models at PP on monthly time scales (Figure 6c), but the importance of volumetric soil moisture (θ) variability on monthly time scales is greater for the sampled time series. Note: θ is of minor importance on weekly time scales at HW. Abbreviations: PP = loblolly pine plantation; HW = mature oak–hickory-dominated hardwood forest; PAR = photosynthetically active radiation; and LAI = leaf area index.

the wider range of environmental conditions experienced by the coniferous ecosystem. The sensitivity of HW to modeling the seasonality of V_{cmax} highlights the large variations in this parameter that result from leaf development, aging and senescence throughout the growing season in some of the species at HW (see Figure 4 in Wilson et al. 2001).

Major simplifications in the temporal and spatial profile of LAD did not compromise spectral fit, and this result is particularly evident at HW, where the diverse canopy structure makes any spatially inexplicit model of LAD a simplification. The simplified canopy profile (LAD_s) at PP fared worse than when using mean LAD. The LAD_s incorporated LAD from only the overstory loblolly pine trees and ignored understory contributions, consequently assuming that all of the leaf area was in the active overstory, and thus overestimated NEE. The added steps of the multilayer A_c model in the model transfer function (Figure 2) may be unnecessary to replicate NEE variability at longer time scales, given that the bulk LAI dynamics may dominate over the precise shape of the LAD profile.

In summary, the A_c component of NEE models was generally amenable to simplifications of the canopy structure and biochemistry, and Figure 9 summarizes the sensitivity analyses by identifying the time scales at which including variability of environmental drivers most impacts the spectral response of the models. The R_E models tested here generally require improvement, possibly by employing nonstationary parameters. In many cases, adding more variables and parameters) did not result in improved spectral fit for the NEE models.

Acknowledgments

This research was supported by the Office of Science (BER), U.S. Department of Energy, Grant No. DE-FG02-00ER63015, by the National Institute of Global Environmental Change (NIGEC) through the Southeast Regional Center at the University of Alabama, Tuscaloosa (DOE cooperative agreement DE-FC030-90ER61010) and by the SERC-NIGEC RCIAP Research Program. We thank K. Wesson, C. Lai, Y. Parashkevov, J. Uebellherr, K. Schäfer, B. Poulter and D. Ellsworth for data collection in the Duke Forest; Richard Mackubin Broadwell and Dan Richter for information on soils; and Min Zhang and David Hollinger for helpful discussions on ecosystem respiration.

References

Andrews, J.A. and W.H. Schlesinger. 2001. Soil CO_2 dynamics, acidification, and chemical weathering in a temperate forest with experimental CO_2 enrichment. Global Biogeochem. Cycles 15:149–162.

Andrews, J.A., K.G. Harrison, R. Matamala and W.H. Schlesinger. 1999. Separation of root respiration from total soil respiration using carbon-13 labeling during Free-Air Carbon Dioxide Enrichment (FACE). Soil Sci. Soc. Am. J. 63:1429–1435.

Aphalo, P.J. and P.G. Jarvis. 1991. Do stomata respond to relative humidity? Plant Cell Environ. 14:127–132.

Baldocchi, D. 1994. An analytical solution for coupled leaf photosynthesis and stomatal conductance models. Tree Physiol. 14: 1069–1079.

Baldocchi, D. and K.B. Wilson. 2001. Modeling CO_2 and water vapor exchange of a temperate broadleaved forest across hourly to decadal time scales. Ecol. Model. 142:155–184.

Baldocchi, D., E. Falge and K.B. Wilson. 2001. A spectral analysis of biosphere–atmosphere trace gas flux densities and meteorological variables across hour to multi-year time scales. Agric. For. Meteorol. 107:1–27.

Ball, J.T., I.E. Woodrow and J.A. Berry. 1987. A model predicting stomatal conductance and its contribution to the control of photosynthesis under different environmental conditions. *In* Progress in Photosynthesis Research. Ed. J. Biggins. M. Nijhoff, Dordrecht, pp 221–224.

Berner, R.A. and A.C. Lasaga. 1989. Modeling the geochemical carbon cycle. Sci. Am. 260:74–81.

Campbell, G.S. and J.M. Norman. 1998. An introduction to environmental biophysics. 2nd Edn. Springer, New York, 286 p.

Collatz, C.J., J.T. Ball, C. Grivet and J.A. Berry. 1991. Physiological and environmental regulation of stomatal conductance, photosynthesis and transpiration: a model that includes a laminar boundary layer. Agric. For. Meteorol. 54:107–136.

Ehleringer, J.R. 1993. Carbon and water relations in desert plants: an isotopic perspective. *In* Stable Isotopes and Plant Carbon–Water Relations. Eds. J.R. Ehleringer, A.E. Hall and G.D. Farquhar. Academic Press, San Diego, pp 155–172.

Ellsworth, D.S. 1999. CO_2 enrichment in a maturing pine forest: are CO_2 exchange and water status in the canopy affected? Plant Cell Environ. 22:461–472.

Ellsworth, D.S. 2000. Seasonal CO_2 assimilation and stomatal limitations in a *Pinus taeda* canopy. Tree Physiol. 20:435–445.

Falge, E., D. Baldocchi, R. Olson et al. 2001. Gap filling strategies for defensible annual sums of net ecosystem exchange. Agric. For. Meteorol. 107:43–69.

Farquhar, G.D., S. von Caemmerer and J.A. Berry. 1980. A biochemical model of photosynthetic CO_2 assimilation in leaves of C_3 species. Planta 149:78–90.

Goulden, M.L., J.W. Munger, S. Fan, B.C. Daube and S. Wofsy. 1996. Measurements of carbon sequestration by long-term eddy covariance: methods and a critical evaluation of accuracy. Global Change Biol. 2:169–182.

Gruber, N., C.D. Keeling and N.R. Bates. 2002. Interannual variability in the North Atlantic Ocean carbon sink. Science 298: 2374–2378.

Horwath, W.R., K.S. Pregitzer and E.A. Paul. 1994. ^{14}C allocation in tree-soil systems. Tree Physiol. 14:1163–1176.

Hsieh, C.I., G. Katul and T. Chi. 2000. An approximate analytical model for footprint estimation of scalar fluxes in thermally stratified atmospheric flows. Adv. Water Resour. 23:765–772.

Hui, D., Y. Luo and G.G. Katul. 2003. Interannual variability in ecosystem respiration and net ecosystem CO_2 exchange in Duke Forest. Tree Physiol. 23:433–442.

Janssens I.A. and K. Pilegaard. 2003. Large seasonal changes in Q_{10} of soil respiration in a beech forest. Global Change Biol. 9: 911–918.

Janssens, I.A., H. Lankreijer, G. Matteucci et al. 2001. Productivity overshadows temperature in determining soil and ecosystem respiration across European forests. Global Change Biol. 7:269–278.

Katul, G. and M.B. Parlange. 1995. Analysis of land surface heat fluxes using the orthonormal wavelet approach. Water Resour. Res. 31:2743–2749.

Katul, G.G. and M.B.S. Siqueira. 2002. Modeling heat, water vapor and CO_2 flux distribution inside canopies using turbulent transport theories. Vadoze Zone J. 1:58–67.

Katul, G., R. Oren, D.S. Ellsworth, C.-I. Hsieh, N. Phillips and K. Lewin. 1997. A lagrangian dispersion model for predicting CO_2 sources, sinks and fluxes in a uniform loblolly pine (*Pinus taeda* L.) stand. J. Geophys. Res. 102:9309–9321.

Katul, G., D.S. Ellsworth and C.T. Lai. 2000. Modeling assimilation and intercellular CO_2 from measured conductance: a synthesis of approaches. Plant Cell Environ. 23:1313–1328.

Katul, G., C.-T. Lai, K.V.R. Schäfer, B. Vidakovic, J.D. Albertson, D.S. Ellsworth and R. Oren. 2001. Multiscale analysis of vegetation surface fluxes: from seconds to years. Adv. Water Resour. 24: 1119–1132.

Keeling, C.D., J.F.S. Chin and T.P. Whorf. 1996. Increased activity of northern vegetation inferred from atmospheric CO_2 measurements. Nature 382:146–149.

Kirschbaum, M.U.F. 1995. The temperature dependence of soil organic matter decomposition, and the effect of global warming on soil organic C storage. Soil Biol. Biochem. 27:753–760.

Kirschbaum, M.U.F. 2000. Will changes in soil organic carbon act as a positive or negative feedback on global warming? Biogeochemistry 48:21–51.

Lai, C.-T. and G. Katul. 2000. The dynamic role of root-water uptake in coupling potential to actual transpiration. Adv. Water Resour. 23:427–439.

Law, B.E., E. Falge, L. Gu et al. 2002. Environmental controls over carbon dioxide and water vapor exchange of terrestrial vegetation. Agric. For. Meteorol. 113:97–120.

Lee, X. 1998. On micrometeorological observations of surface–air exchange over tall vegetation. Agric. For. Meteorol. 91:39–49.

Lee, X., H.-J. Wu, J. Sigler, A.C. Oishi and T. Siccama. 2004. Rapid and transient response of soil respiration to rain. Global Change Biol. 10:1017–1026.

Leuning, R. 1995. A critical appraisal of a combined stomatal-photosynthesis model for C_3 plants. Plant Cell Environ. 18:339–355.

Lloyd, J. and J.A. Taylor. 1994. On the temperature dependence of soil respiration. Funct. Ecol. 8:315–323.

Moncrieff, J.B., Y. Mahli and R. Leuning. 1996. The propagation of errors in long-term measurements of land–atmosphere fluxes of carbon and water. Global Change Biol. 2:231–240.

Monteith, J.L. 1995. A reinterpretation of stomatal responses to humidity. Plant Cell Environ. 18:357–364.

Mortazavi, B., J.P. Chanton, J.L. Prater, A.C. Oishi, R. Oren and G.G. Katul. 2005. Temporal variability in ^{13}C of respired CO_2 in a pine and a hardwood forest subject to similar climatic conditions. Oecologia 142:57–69.

Naumburg, E., D.S. Ellsworth and G.G. Katul. 2001. Modeling daily understory photosynthesis of species with differing photosynthetic light dynamics in ambient and elevated CO_2. Oecologia 126: 487–499.

Norman, J.M. 1982. Simulation of microclimates. *In* Biometeorology and Integrated Pest Management. Eds. J.L. Hatfield and I. Thompson. Academic Press, New York, pp 65–99.

Novick, K.A., P.C. Stoy, G.G. Katul, D.S. Ellsworth, M.B.S. Siqueira, J. Juang and R. Oren. 2004. Carbon dioxide and water vapor exchange in a warm temperate grassland. Oecologia 138: 259–274.

Ollinger, S.V., J.D. Aber and C.A. Federer. 1998. Estimating regional forest productivity and water yield using an ecosystem model linked to a GIS. Landscape Ecol. 13:323–334.

Olson, J.S., R.M. Garrels, R.A. Berner, T.V. Armentano, M.I. Dyer and D.H. Yaalon. 1985. The natural carbon cycle. *In* Atmospheric Carbon Dioxide and the Global Carbon Cycle. DOE/ER-0239. Ed. J.R. Trabalka. U.S. Department of Energy, Washington, DC, pp 175–213.

Oosting, H.J. 1942. An ecological analysis of the plant communities of Piedmont, North Carolina. Am. Midl. Nat. 28:1–126.

Oren, R. and D.E. Pataki. 2001. Transpiration in response to variation in microclimate and soil moisture in southeastern deciduous forests. Oecologia 127:549–559.

Oren, R., B.E. Ewers, P. Todd, N. Phillips and G. Katul. 1998. Water balance delineates the soil layer in which moisture affects canopy conductance. Ecol. Appl. 8:990–1002.

Oren, R., J.S. Sperry, G. Katul, D.E. Pataki, B.E. Ewers, N. Phillips and K.V.R. Schäfer. 1999. Survey and synthesis of intra- and interspecific variation in stomatal sensitivity to vapor pressure deficit. Plant Cell Environ. 22:1515–1526.

Palmroth, S., C.A. Maier, H.R. McCarthy, A.C. Oishi, H.-S. Kim, K. Johnsen, G.G. Katul and R. Oren. 2005. Contrasting responses to drought of forest floor CO_2 efflux in a loblolly pine plantation and a nearby oak–hickory forest. Global Change Biol. 11: 421–434.

Pataki, D.E. and R. Oren. 2003. Species differences in stomatal control of water loss at the canopy scale in a mature bottomland deciduous forest. Adv. Water Resour. 26:1267–1278.

Pataki, D.E., J.R. Ehleringer, L.B. Flanagan, D. Yakir, D.R. Bowling, C.J. Still, N. Buchmann, J.O. Kaplan and J.A. Berry. 2003. The application and interpretation of Keeling plots in terrestrial carbon cycle research. Global Biogeochem. Cycles 17(1), 1022, doi:10.1029/2001GB001850.

Raich, J.W. and W.H. Schlesinger. 1992. The global carbon dioxide flux in soil respiration and its relationship to vegetation and climate. Tellus Ser. B Chem. Phys. Meteorol. 44:81–99.

Reichstein, M., A. Rey, A. Freibauer et al. 2003. Modeling temporal and large-scale spatial variability of soil respiration from soil water availability, temperature and vegetation productivity indices. Global Biogeochem. Cycles 17:1104.

Scanlon, T.M. and J.D. Albertson. 2001. Turbulent transport of carbon dioxide and water within vegetation canopies during unstable conditions: identification of episodes using wavelet analysis. J. Geophys. Res 106:7251–7262.

Schäfer, K.V.R., R. Oren, D.S. Ellsworth, C.T. Lai, J.D. Herrick, A.C. Finzi, D.D. Richter and G.G. Katul. 2003. Exposure to an enriched CO_2 atmosphere alters carbon assimilation and allocation in a pine forest ecosystem. Global Change Biol. 9:1378–1400.

Schimel, D.S., J.I. House, K.A. Hibbard et al. 2001. Recent patterns and mechanisms of carbon exchange by terrestrial ecosystems. Nature 414:169–172.

Slaytor, A. 1906. Studies in fermentation. I. The chemical dynamics of alcoholic fermentation by yeast. J. Chem. Soc. 89:136–142.

Swanson, R.V. and L.B. Flanagan. 2001. Environmental regulation of carbon dioxide exchange at the forest floor in a boreal black spruce ecosystem. Agric. For. Meteorol. 108:165–181.

Torrence, C. and G.P. Compo. 1998. A practical guide to wavelet analysis. Bull. Am. Meteorol. Soc. 79:61–78.

van't Hoff, J.H. 1884. Études de dynamique chemique. Frederik Müller and Co., Amsterdam, 214 p.

Webb, E.K., G.I. Pearman and R. Leuning. 1980. Correction of flux measurements for density effects due to heat and water vapour transfer. Q. J. R. Meteorol. Soc. 106:85–100.

Wilson, K.B., D.D. Baldocchi and P.J. Hanson. 2001. Leaf age affects the seasonal pattern of photosynthetic capacity and net ecosystem exchange of carbon in a deciduous forest. Plant Cell Environ. 24: 571–583.

Winkler, J.P., R.S. Cherry and W.H. Schlesinger. 1996. The Q_{10} relationship of microbial respiration in a temperate forest soil. Soil Biol. Biochem. 28:1067–1072.

Appendix A: Ecosystem respiration models

We briefly describe additions to the "Q_{10}" R_E model (Equation 1) that account for potential effects of θ, LAI and recently assimilated carbon on R_E.

Various models have been used to describe the relationship between θ and R_E, and results appear to be highly site specific. Volumetric soil water influences R_E by reducing plant and microbial activity under dry conditions, and by inhibiting O_2 diffusion and thus microbial function under wet conditions. We used a function, $f(\theta)$, that adjusts R_E down during dry and wet periods while retaining temperature sensitivity across the range of intermediary θ:

$$f(\theta) = -\frac{1}{e} + \frac{\exp\left(-\left|\left(\frac{\theta - a}{b}\right)^m\right|\right)}{1 - \frac{1}{e}} \quad \text{(A1)}$$

The three fitted parameters, a, b and m, adjust the point along the θ scale at which the function reaches its maxima, the slope of the tails, and the shape of the tails, respectively (Figure A1). The model $R_{E\theta}$ is obtained by multiplying Equation 1 by Equation A1 (Table 1).

Standing biomass and productivity are important determinants of R_E at PP and HW (Janssens et al. 2001, Pataki et al. 2003, Mortazavi et al. 2005). The effects of respiring biomass and recently assimilated carbon on R_E can be modeled hierarchically where Q_{10} model parameters are a function of respiring biomass, A_c, or environmental drivers, or by adding additional terms to the R_E model. To keep the analysis simple, we chose the latter. We took LAI to be a surrogate for respiring biomass and added a linear model component (after Reichstein et al. 2003) to R_{EQ10}a:

$$R_{ELAI} = R_{10} Q_{10}^{(T_a - 10)/10} + c\text{LAI} + d \quad \text{(A2)}$$

where c and d are fitted parameters.

It is difficult to determine the effects of A_c on R_E using EC because A_c is not measured directly. The sum of daytime NEE was used as a surrogate for A_c, and data from the literature were used to estimate the optimum window to account for the effects of A_c on R_E. Andrews et al. (1999) found that respired CO_2 in the top 15 cm of soil was depleted in ^{13}C within 1 week of fumigation in the ^{13}C-labeled elevated CO_2 rings of the FACE experiment at PP. Root respiration of assimilates can occur within 12 h as evidenced by ^{14}C analysis of 3-m-tall *Populus* trees, for which the ^{14}C pulse effect was negligible after 2 weeks (Horwath et al. 1994). Four days was a sufficient window to identify the effect of VPD on δC^{13} through its effect on stomatal conductance and A_c at PP and HW (Mortazavi et al. 2005). Thus, the 2-week cumulative sum of NEE (NEE_{cum}) was considered to be a conservative window for modeling the effects of carbon assimilation on R_E for both ecosystems, and the model R_{EAc} takes the same form as Equation A2:

$$R_{EAc} = R_{10} Q_{10}^{(T_a - 10)/10} + h\text{NEE}_{cum} + j \quad \text{(A3)}$$

where h and j are fitted parameters.

In addition to the above R_E model improvements, we tested two variations of the Q_{10} model where the parameters are fit for combined summer and winter periods (abbreviated R_{EVP1}), or for each summer and winter period separately (R_{EVP2}). These models are meant to resemble a hierarchical model structure, where independent variables influence the parameters of a structurally simple model.

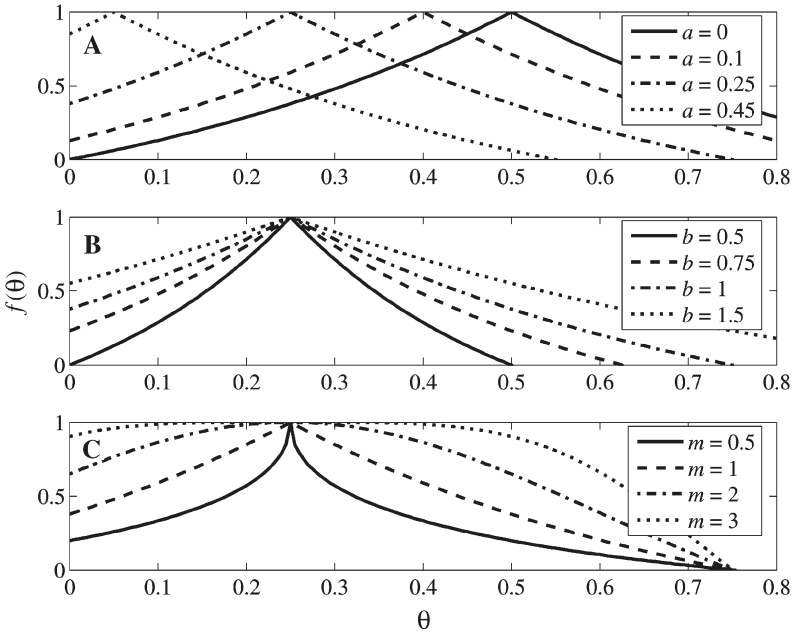

Figure A1. The shape of $f(\theta)$ from Equation A1 for different a "scale" (A), b "slope" (B) and m "shape" (C) parameters.

Appendix B: Farquhar photosynthesis model

The Farquhar model is described in detail elsewhere (Farquhar et al. 1980, Collatz et al. 1991). Briefly, leaf-level photosynthesis is the product of a system of multiple limitations arising primarily from light-driven electron transport (J_E) or ribulose biphosphate carboxylase-oxygenase (Rubisco) activity (J_C). Thus:

$$A_c = \min\begin{pmatrix} J_E \\ J_C \end{pmatrix} \tag{B1}$$

$$J_E = \alpha e_m \mathrm{PAR}_i \frac{C_i - \Gamma}{C_i + 2\Gamma} \tag{B2}$$

$$J_C = \frac{V_{cmax}(C_i - \Gamma)}{C_i + K_{CO_2}\left(1 + \frac{O_2}{K_{O_2}}\right)} \tag{B3}$$

where α is leaf PAR absorptivity, e_m is maximum quantum efficiency for CO_2 uptake, and PAR_i is PAR at canopy layer i. We used a simple light attenuation model after Campbell and Norman (1998) to model PAR_i without consideration of sunlit and shaded foliage or any penumbral effects. Parameter Γ is the leaf CO_2 compensation point as in Equation 5, O_2 is atmospheric O_2 concentration, V_{cmax} is maximum Rubisco activity per unit leaf area, and K_j describes a temperature-dependent kinetic parameter that takes the form:

$$K_j = K_{j,25} \exp(\gamma(T_L - 25)) \tag{B4}$$

where the subscript j refers to either CO_2 or O_2, $K_{j,25}$ is the parameter value at 25 °C, γ is a temperature coefficient and T_a was used to approximate leaf temperature T_L. We used general Farquhar parameter values from Campbell and Norman (1998) and tested model sensitivity to the temperature dependence (Equation B4) and seasonal variations in the V_{cmax} parameter. At PP, seasonal trends in $V_{cmax,25}$ were taken from other studies conducted at the site (Ellsworth 2000). At HW, temporal variations in $V_{cmax,25}$ were assumed to follow the relationship between leaf age and V_{cmax} (Wilson et al. 2001). Measured V_{cmax} (Naumburg et al. 2001) was used for understory species in both ecosystems.